

Results from a Prototype Chicane-Based Energy Spectrometer for a Linear Collider

A. Lyapin^{a,*}, H.J. Schreiber^b, M. Viti^b, C. Adolphsen^c, R. Arnold^c,
S. Boogert^d, G. Boorman^d, M. V. Chistiakova^h, F. Gournaris^a,
V. Duginov^e, C. Hast^c, M. Hildreth^g, C. Hlaing^h, F. Jacksonⁱ,
O. Khainovsky^h, Yu. G. Kolomensky^h, S. Kostromin^e, K. Kumar^c,
B. Maiheu^a, D. McCormick^c, D. J. Miller^a, N. Morozov^e, T. Orimoto^{h,j},
E. Petigura^h, M. Sadre-Bazzaz^h, M. Slater^f, Z. Szalata^c, M. Thomson^f,
D. Ward^f, M. Wendt^k, M. Wing^a, M. Woods^c

^aUniversity College London, London, UK

^bDeutsches Elektronen Synchrotron DESY Hamburg and Zeuthen, Germany

^cSLAC National Accelerator Laboratory, Menlo Park, California, USA

^dRoyal Holloway, University of London, Egham, UK

^eJoint Institute for Nuclear Research, Dubna, Moscow Region, Russia

^fUniversity of Cambridge, Cambridge, UK

^gUniversity of Notre Dame, Notre Dame, Indiana, USA

^hUniversity of California and Lawrence Berkeley National Laboratory, Berkeley,
California, USA

ⁱDaresbury Laboratory, Daresbury, UK

^jCalifornia Institute of Technology, Pasadena, California, USA

^kFermi National Accelerator Laboratory, Batavia, Illinois, USA

Abstract

The International Linear Collider and other proposed high energy e^+e^- machines aim to measure with unprecedented precision Standard Model quantities and new, not yet discovered phenomena. One of the main requirements for achieving this goal is a measurement of the incident beam energy with an uncertainty close to 10^{-4} . This article presents the analysis of data from a prototype energy spectrometer commissioned in 2006–2007 in SLAC’s End Station A beamline. The prototype was a 4-magnet chicane equipped with beam position monitors measuring small changes of the beam orbit through the chicane at different beam energies. A single bunch energy resolution close to $5 \cdot 10^{-4}$ was measured, which is satisfactory for most scenarios. We also report on the operational experience with the chicane-based spectrometer and suggest ways of improving its performance.

Preprint submitted to Nuclear Instruments and Methods in Physics Research Section A
6BT, London, United Kingdom. Tel: +44 (0)20 7679 3454; Fax: +44 (0)20 7679 7145.

Email address: al@hep.ucl.ac.uk (A. Lyapin)

¹This work was supported by the Commission of the European Communities under the 6th Framework Programme “Structuring the European Research Arm,” contract number RIDS-011899 and by the Science and Technology Facilities Council (STFC)

²This work was supported by the U.S. Department of Energy under contract DE-AC02-76SF00515

³This work was supported by the U.S. Department of Energy under contract DE-FG02-03ER41279

35 *Keywords:* Energy measurement, Energy Spectrometer, Cavity Beam
36 Position Monitor, BPM, End Station A, ESA, International Linear
37 Collider, ILC

38 1. Introduction

39 The physics potential of the next e^+e^- Linear Collider depends greatly
40 on precision energy measurements of the electron and positron beams at the
41 interaction point (IP). Beam energy measurements are mandatory for the
42 precision determination of the fundamental properties of particles created in
43 the processes of interest. For example, measuring the top mass to order of
44 100 – 200 MeV or measuring the mass of the Standard Model Higgs boson
45 to about 50 MeV using the Higgs-strahlung process requires the luminosity-
46 weighted collision energy to be known to a level of $(1 - 2) \cdot 10^{-4}$ to avoid this
47 being the dominant uncertainty [1].

48 The strategy proposed in the International Linear Collider (ILC) design
49 report [2] is to have redundant beam-based measurements capable of achiev-
50 ing a 10^{-4} relative precision on a single beam, which would be available in
51 real time as a diagnostic tool to the operators. Also, physics reference chan-
52 nels, such as $e^+e^- \rightarrow \mu^+\mu^-\gamma$, where the muons are resonant with the known
53 Z-mass, are expected to provide valuable cross-checks of the collision energy
54 scale, but only long after the data have been recorded.

55 The primary method planned to perform E_b measurements at the ILC is
56 a non-invasive energy spectrometer using beam position monitors (BPMs).
57 The proposed setup is similar to that used for calibrating the energy scale for
58 the W-mass measurement at LEP-II [3]. At the ILC, however, the parame-
59 ters of the spectrometer are tightly constrained to provide limited emittance
60 dilution at the highest ILC energy $E_b = 500$ GeV.

61 Initially, a 3-magnet chicane located upstream of the interaction point
62 just after the energy collimators of the beam delivery system (BDS) was
63 proposed [4]. However, the baseline ILC spectrometer design uses two dipole
64 magnets to produce a beam displacement x , while two more magnets return
65 the beam to the nominal beam orbit. For such a chicane, the beam energy
66 (to first order) is then given by

$$E_b = \frac{c \cdot e \cdot L}{x} \int_{\text{magnet}} B \, dl, \quad (1)$$

67 where L is the distance between the first two magnets, $\int B dl$ the integral
68 of the magnetic field in each magnet, c the speed of light and e the electric
69 charge of the electron.

70 The 4-magnet chicane avoids spurious beam displacement signals in the
71 BPMs due to the inclination of the beam trajectory, and thus systematic
72 errors in E_b measurements. For this reason, a 4-magnet spectrometer, which
73 maintains the beam axially with respect to the axis of the cavity BPMs,
74 seems preferable to a more conventional 3-magnet chicane. In both cases the
75 magnetic field in the spectrometer chicane can be recorded and reversed for
76 studying systematic effects without changing the beam direction downstream
77 of the spectrometer.

78 A dispersion of 5 mm at the centre of the chicane can be introduced
79 routinely without a significant degradation of the beam emittance due to
80 synchrotron radiation. When operating a fixed dispersion of 5 mm over the
81 whole energy range, a BPM resolution better than $0.5 \mu\text{m}$ is needed. This
82 resolution can be achieved with cavity BPMs [5]. Since the spectrometer
83 bending magnets need to operate at low fields when running the ILC at
84 the Z-pole, the magnetic field measurement may not be accurate enough
85 to provide the required level of precision. A significantly improved BPM
86 resolution would, however, allow the magnets to be run at the same field for
87 both the Z-pole and highest energy operation.

88 Some original energy resolution studies of the SLAC prototype 4-magnet
89 chicane were presented in ref. [6]. The analysis used calibrated beam position
90 readings but revealed that due to small differences between the magnets in
91 the chicane the beam inclination also needs to be considered. The analysis
92 has here been extended by using complex BPM readings that contain the in-
93 formation on both the beam offset and inclination. This approach eliminates
94 the need for position calibration of the BPMs, while the whole system can
95 be calibrated by means of an energy scan.

96 In this publication we estimate the resolution of the spectrometer to com-
97 pare it with the result of $8.5 \cdot 10^{-4}$ measured in [6]. We also consider the im-
98 pact of different systematics on the energy measurement in order to improve
99 the resolution to the 10^{-4} level in future experiments.

100 **2. Test Beam Setup and Spectrometer Hardware Configuration**

101 A prototype test setup for a 4-magnet chicane was commissioned in 2006
102 (the T-474 experiment) and extended in 2007 (the T-491 experiment) in the

103 End Station A (ESA) beamline at the SLAC National Accelerator Labora-
104 tory [7].

105 In our experiments the electron beam generated by the main Linear Ac-
106 celerator at SLAC was transported to the ESA experimental area through
107 the 300 m long A-line, which includes bending and focusing magnets, diag-
108 nostic instruments, such as stripline and RF cavity BPMs, charge sensitive
109 toroids, a synchrotron light monitor, profile screens and diodes. The SLAC
110 linac provided single bunches at 10 Hz and a nominal energy of 28.5 GeV, a
111 bunch charge of $1.6 \cdot 10^{10}$ electrons, a bunch length of 500 μm and an energy
112 spread of 0.15%, i.e. a beam with properties similar to the ILC expectations
113 at the highest energy currently available for electrons.

114 These beam parameters allowed us to test the capabilities of the proposed
115 spectrometer under realistic conditions. Two feedback systems were in place
116 for the ESA beam: one for its position and one for the energy. The position
117 feedback stabilised the beam position and angle using cavity BPMs and cor-
118 rector magnets upstream of the ESA area. The energy feedback stabilised
119 the energy by controlling the phase of the klystrons, and thus the accelerat-
120 ing gradient, in one of the linac sections. The energy feedback was also used
121 for offsetting the energy from the nominal value in approximately 50 MeV
122 steps within a ± 100 MeV range, thus providing a rough energy calibration
123 for the spectrometer.

124 Remaining beam energy drifts change the beam orbit through the transfer
125 line, resulting in increased beam losses as the trajectory wanders off the op-
126 timal one. Monitoring these losses and correcting for the drifts manually, the
127 linac operators kept the beam energy within a $\pm 1\%$ range around 28.5 GeV
128 during the run.

129 The setup, as schematically shown in fig. 1, includes four bending magnets
130 denoted as 3B1, 3B2, 3B3 and 3B4, forming a chicane in the horizontal plane
131 and high-precision cavity BPMs upstream, downstream and in between the
132 dipole magnets. Two of them (BPMs 4 and 7) in the middle of the chicane
133 were instrumented with precision movers. When the magnets were turned
134 on, these BPMs were mechanically moved to ensure the beam offset fits the
135 dynamic range of the BPM electronics. These movers were also used for
136 position calibrations. Horizontal positions of three BPMs (3, 4 and 7) were
137 monitored with a Zygo interferometer [8].

138 The 10D37 magnets from the old SPEAR injection beamline, refurbished
139 for the use in the chicane, are 37" long, 10" wide on the pole faces and have
140 a 3" gap. They were run in series from a single power supply to minimise

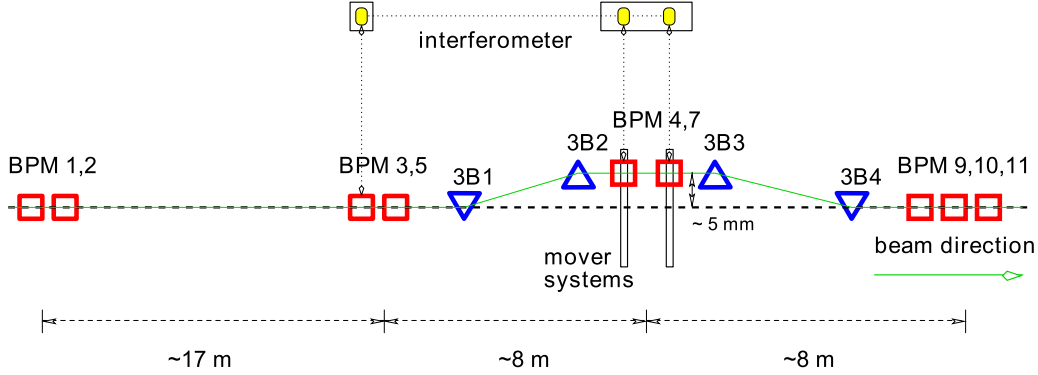


Figure 1: Schematic representation of the prototype spectrometer in ESA.

141 relative drifts. The magnets were studied during a set of measurements in
 142 the SLAC Magnet Measurement Laboratory. Magnetic field maps of the
 143 vertical field component B_y were taken using NMR and Hall probes, while
 144 each $\int B dl$ was measured using a flip coil, which was calibrated against a
 145 moving wire system. Stability and reproducibility were at the focus of these
 146 measurements. Details of the field measurements can be found in [6, 9, 10].

147 In situ at ESA, two NMR probes with different, but overlapping working
 148 ranges and initially also one Hall probe were installed in the first magnet 3B1,
 149 while one NMR probe was positioned in each of the other three magnets, so
 150 that field integral values could be monitored. In the test data runs, the
 151 nominal magnetic field integral was set at 0.117 T·m, which corresponds to
 152 a current of 150 A. The stray field outside the magnets in the middle of
 153 the chicane was monitored using two low-field fluxgate magnetometers. One
 154 was placed on the girder to obtain the horizontal (x) and vertical (y) field
 155 components and the other on the beam pipe measuring the y -component
 156 only. Properties of the probes and the fluxgate monitors are summarised in
 157 fig. 2.

158 The readout unit for the NMR probes provided one internally-averaged
 159 reading every 2.5 s. The probes were multiplexed, sharing the same readout.
 160 Typically 9 readings were obtained for each probe before switching to the
 161 next probe, totalling an observation time of about 20 s. The gap between
 162 observations, while other probes were read out, was about one minute, while
 163 an energy scan took about 3 minutes at 10 Hz beam repetition frequency.
 164 Therefore, only slow (compared to the data rate) variations of the magnetic

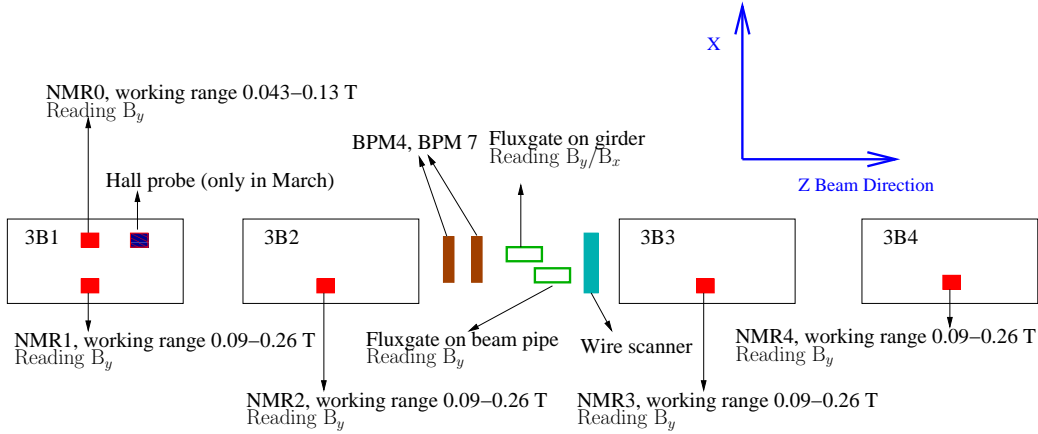


Figure 2: Magnetic field diagnostics in the spectrometer chicane.

165 field could be tracked reliably.

166 In order to measure the beam orbit, 8 cavity BPMs, all operating in
 167 the RF S-band, were installed. Three of them were SLAC prototype ILC
 168 BPMs (3, 4, 5) using cylindrical cavities with x - and y -waveguides for the
 169 dipole mode coupling and monopole mode suppression. Each of the five
 170 SLAC BPMs (A-line-type BPMs 1 and 2, and linac-type BPMs 9, 10, and
 171 11) consists of three cavities: two rectangular cavities for x and y separately
 172 to avoid x - y couplings, and one cylindrical cavity to provide charge and
 173 phase information [11]. BPM 7 was a dedicated ILC prototype designed and
 174 manufactured in the UK for the use in the spectrometer. Unfortunately, this
 175 monitor could not be used in the analysis due to manufacturing problems [12].
 176 Micrometre level resolution was measured for BPMs 1 and 2, while BPMs
 177 3, 4, 5, 9, 10 and 11 demonstrated a resolution below $1 \mu\text{m}$. Details on the
 178 performance of the BPM system and the A-line configuration can be found
 179 in [5].

180 BPMs 12 and 24 are placed in the bending arc region of the A-line, where
 181 horizontal dispersion reaches about 0.5 m. For our experiment they were
 182 instrumented with the same high-sensitivity electronics as all other BPMs in
 183 the ESA beamline, so that the energy measurements in the A-line and in the
 184 chicane could be performed simultaneously and cross-checked against each
 185 other.

186 **3. Performance of the Prototype Spectrometer**

187 *3.1. Reconstruction of the beam orbit in the middle of the chicane*

188 As the chicane magnets bend the beam in the x -direction, we are mainly
189 interested in the horizontal beam position and angle, and, unless specified
190 otherwise, we refer to the x -coordinate throughout this section.

191 In our system, signals generated by the BPMs were digitised and stored
192 in data files for each event, i.e. for each beam trigger. They are digitally
193 demodulated in the analysis [5]. A complex digital local oscillator signal
194 allows decoding of both the amplitude and the phase of the signal's phasor
195 along the waveform. Sampled at a point close to the peak and normalised by
196 the phasor from the reference cavity, the converted waveforms give the real,
197 in-phase (I), value and the imaginary, quadrature (Q), value, which contain
198 the information on the beam offset as well as the inclination.

199 The offset of the beam trajectory in the middle of the chicane has to
200 be measured with respect to the nominal orbit position reconstructed using
201 BPMs outside of the chicane. In order to form a prediction of the beam
202 position at the BPM 4 location we took data with zero current in the magnets
203 and selected a "quiet period", when neither the beam nor the hardware
204 settings were altered. We then correlated the I and Q readings of BPM 4
205 with the data from other BPMs. Forming the prediction can be visualised
206 as continuing the beam trajectory line connecting the points measured by
207 other BPMs up to BPM 4 location. The best set of correlation coefficients
208 minimizes the offset between that line and the measured points for the
209 majority of the beam passes.

210 Data from a run with magnets on could also be used for relative measure-
211 ments and would result in a better prediction, however, due to the residual
212 dispersion in the beamline, beam positions before and in the middle of the
213 chicane are correlated. Hence, only data from a run with magnets off were
214 used.

215 BPMs 9, 10 and 11 were not used for the prediction because, when mag-
216 nets are on, the impact of the chicane on the beam orbit is not fully com-
217 pensated, and the beam offset in these BPMs is energy-correlated.

218 Due to alignment errors, there is also a correlation between the vertical
219 beam position and angle before the chicane and the horizontal beam position
220 and angle in the mid-chicane. Therefore, both x - and y -readings from the
221 BPMs upstream of the chicane (x_1 , x_2 , x_3 , x_5 , y_1 , y_2 , y_3 and y_5) were used
222 in the analysis.

223 In order to reconstruct the beam orbit in the mid-chicane, the I and Q
 224 values from BPM 4 are correlated to the I and Q values from the upstream
 225 BPMs. We applied the Singular Value Decomposition (SVD) method [13] to
 226 several thousands of readings. Inversion of the matrix of the measured I and
 227 Q values for the selected BPMs provides a vector of coefficients, which relate
 228 the Is and Qs of each BPM, i , to those of BPM 4 so that a prediction can
 229 be made:

$$I_{\text{BPM4}} = \alpha_0 + \sum_i \alpha_i^{(I)} \cdot I_i + \sum_i \alpha_i^{(Q)} \cdot Q_i, \quad (2)$$

$$Q_{\text{BPM4}} = \beta_0 + \sum_i \beta_i^{(I)} \cdot I_i + \sum_i \beta_i^{(Q)} \cdot Q_i, \quad (3)$$

230 where $\alpha_{0,i}$ and $\beta_{0,i}$ are the SVD coefficients.

231 The difference between the predicted and the measured values is the resid-
 232 ual. In our case, the RMS residual is the precision of the orbit prediction
 233 and the resolution of BPM 4 added in quadrature. It sets the limit on the
 234 spectrometer resolution. The measured and predicted values for I and Q are
 235 plotted against each other in fig. 3. The points in these plots lie around
 236 the $y = x$ solid lines, which means the prediction works correctly. The his-
 237 tograms in the bottom part of fig. 3 show the residuals, for both the I and
 238 Q values.

239 It is clear that the I and Q residuals for BPM 4 are small compared to
 240 the average I and Q values, but the results in fig. 3 are still hard to interpret
 241 quantitatively. In order to set the scale we used the mover scan data. During
 242 the mover scan BPM 4 was moved in 0.25 mm steps from -0.5 to $+0.5$ mm off
 243 the nominal position. The precision of the mover system is about $10 \mu\text{m}$, but
 244 the moves can also be observed by the interferometer with a sub-micrometre
 245 precision. Fig. 4 shows the scan data as well as the position residual, which
 246 was calculated for the data used in the SVD computations above. A position
 247 residual of $2.73 \mu\text{m}$ was determined, which is close to the estimate in [6]
 248 ($2.3 \mu\text{m}$).

249 The residual is larger than our earlier published value [5], which was close
 250 to $1 \mu\text{m}$. This is due to the movement of BPM 4 from its original location
 251 between BPMs 3 and 5 to the middle of the chicane and exclusion of BPMs
 252 9, 10 and 11 from this analysis. Therefore, BPM 4, which was previously in
 253 the “centre of gravity”, here is at the edge of the BPM system. Clearly, the
 254 precision of the orbit reconstruction at BPM 4 was affected.

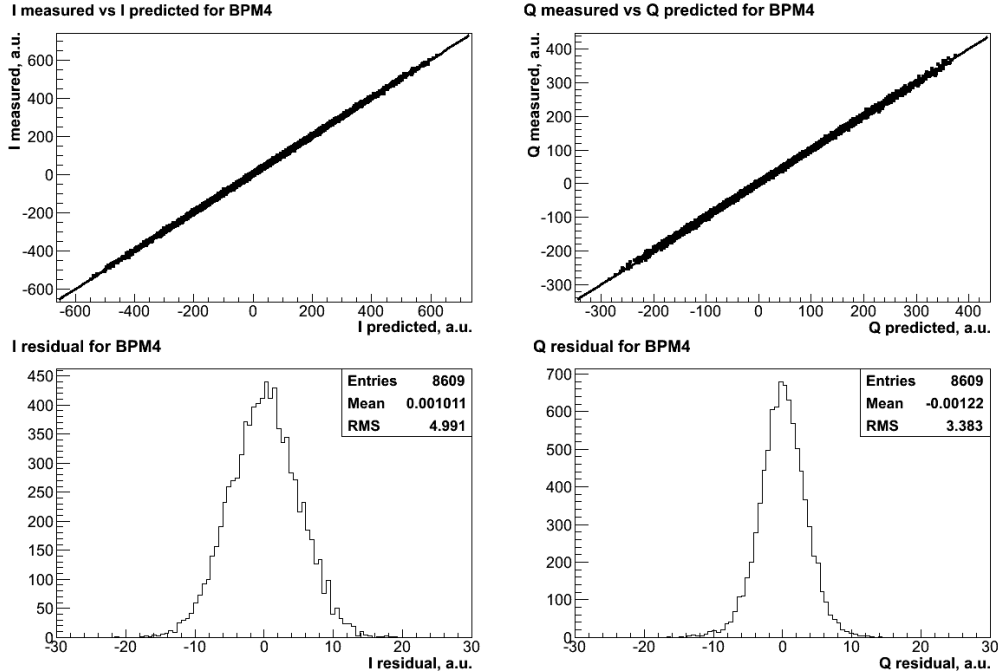


Figure 3: BPM 4 readings predicted from other BPMs in the beamline: I predicted vs I measured (top left), Q predicted vs Q measured (top right), I residual (bottom left), Q residual (bottom right).

255 Together with the 5 mm nominal beam offset in the middle of the chicane
 256 for magnets on, the $2.73 \mu\text{m}$ precision of the BPM system sets an energy
 257 resolution limit of $5.5 \cdot 10^{-4}$ for our spectrometer prototype.

258 3.2. Estimate of the beam energy and scale correction

259 The I and Q readings predicted for BPM 4 by all other BPMs can be
 260 subtracted from the measured values and, when the magnets are on, provide
 261 information on how the beam trajectory changes with the energy.

262 When turning the magnets on, we also moved BPM 4 by 5 mm in order to
 263 keep the beam centred. This movement was observed by the Zygo interferom-
 264 eter. According to the interferometer, BPM 4 moved by 5.0034 mm between
 265 our selected runs with magnets on and magnets off. Using the IQ rotation
 266 and scale from the mover scan, we can predict the changes of the I and Q val-
 267 ues of BPM 4. This results in offsets of $I_0 = -8784$ and $Q_0 = -4605$, which

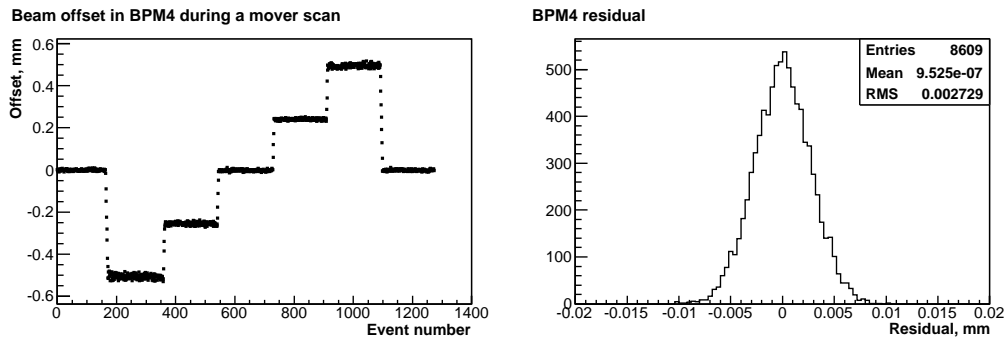


Figure 4: BPM 4 position for a horizontal mover scan (left), BPM 4 residual during a quiet period (right).

268 were added to the I and Q values from the energy scan after the predictions
 269 had been subtracted (fig. 5, top left).

270 Although a small inclination of the beam orbit is introduced along with
 271 the offset in the middle of the chicane due to small differences between the
 272 magnets, the measured points still lie on a straight line in the IQ plane as
 273 both the offset and inclination scale with the energy. Fitting the measured
 274 data to a straight line going through the centre of coordinates, we obtain the
 275 IQ rotation of this “energy line”. Energy readings for each point are then
 276 calculated as a projection onto the energy line.

277 In order to compute the energy scale, individual readings are averaged
 278 for each step of the energy scan and then fitted to a straight line (fig. 5,
 279 top right). The slope of this line gives the energy scale and the offset – the
 280 measured nominal energy. This procedure results in a beam energy of about
 281 32.6 GeV, while, as mentioned above, it was kept within $\pm 1\%$ off 28.5 GeV
 282 during the run. Although the fit may contribute up to 1.4 GeV uncertainty,
 283 introduced by the drifts during the energy scan, the difference is mainly due
 284 to the scale of the energy feedback, which was not re-calibrated for the run.

285 Introducing the values for the total beam offset $x = 5.117$ mm, distance
 286 between the magnets $L = 4.014$ m, and magnetic field integral $\int Bdl =$
 287 0.117 T·m into eq. (1) results in a value lower than expected, 27.5 GeV.
 288 Nevertheless, this estimate confirms that the beam energy was not as high
 289 as measured using the uncorrected energy feedback scale. As measuring the
 290 absolute beam energy is out of the scope of this study, and some systematic
 291 offsets may contribute to E_b , we assume a nominal beam energy of 28.5 GeV

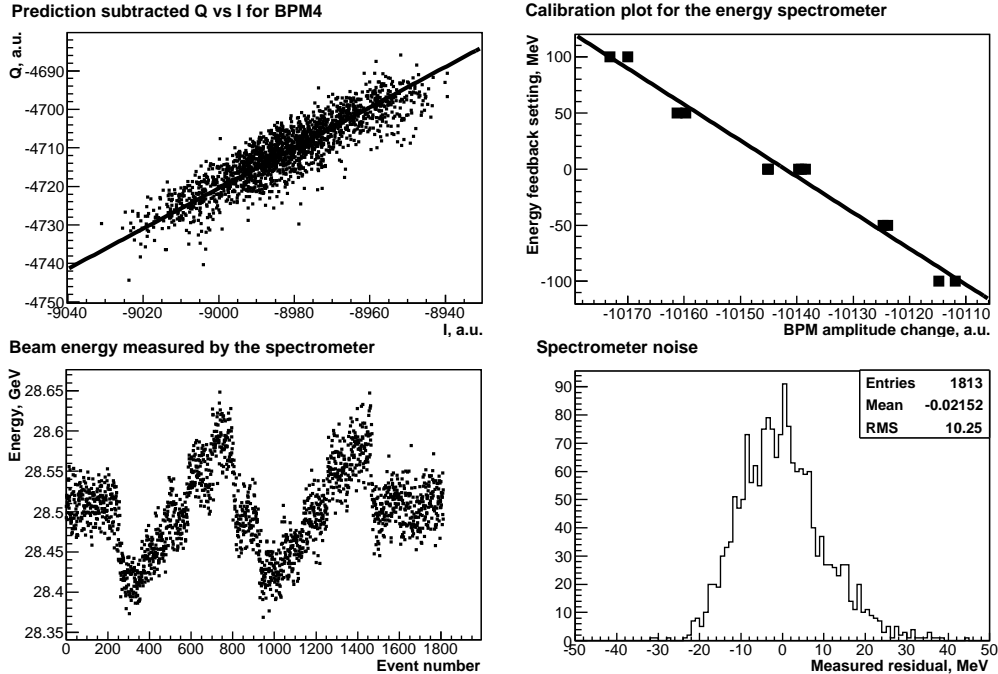


Figure 5: Beam energy measurements: prediction subtracted Q vs I for BPM 4 (offset by Q_0 and I_0 to take into account the 5.0034 mm move), with a fit to the data shown (top left), energy calibration plot for the spectrometer (top right), beam energy measured during the scan (bottom left), spectrometer noise measured off the energy line (bottom right).

292 in this article.

293 The ratio $28.5/32.6$ gives a correction factor of 0.87, meaning that the en-
 294 ergy scan was actually performed in a range of ± 87 MeV instead of requested
 295 ± 100 MeV, and the energy scale factor must be corrected accordingly.

296 The energy measured by BPM 4 during the scan is shown in fig. 5, bottom
 297 left. Peak fluctuations are less or comparable with the energy scan step size
 298 of 50 MeV, so a resolution better than 25 MeV can be expected. In the
 299 following we use the data from the energy BPMs in order to separate the
 300 energy fluctuations from noise, and include additional data acquired with the
 301 setup, such as interferometer and NMR readings, to refine the measurement
 302 and estimate the resolution of the spectrometer.

303 The last plot in fig. 5 (bottom right) shows the distribution of the offsets
 304 of the measured points from the fitted line. The RMS of the distribution is

305 10 MeV, or 8.7 MeV ($3.1 \cdot 10^{-4}$) taking into account the scale correction. This
306 value reflects the noise performance of the BPM system since the energy- and
307 position-induced changes act along the energy line (the incline, although not
308 always negligible, is very small). However, it does not include the effect of
309 the magnetic field, beam position fluctuations and associated non-linearities.
310 Indeed, the resolution estimate of $5.5 \cdot 10^{-4}$ obtained using position data (see
311 section 3.1) is larger.

312 *3.3. Resolution of the energy BPMs*

313 We could only perform a relative energy measurement with BPMs 12
314 and 24, as the field of the bending magnets in the A-line could not be turned
315 off. However, we were still able to calibrate the energy BPMs using the energy
316 scan data and taking into account the energy feedback scale correction.

317 Similarly to spectrometer data, we measured the RMS residual between
318 the fitted energy line and the measured points for the energy BPMs 12 and 24.
319 The measured noise is equivalent to 0.36 MeV for BPM 12 and 2.0 MeV for
320 BPM 24, or $1.3 \cdot 10^{-5}$ and $7.0 \cdot 10^{-5}$ respectively, at the nominal beam energy
321 of 28.5 GeV. The values are different because BPM 12 had an additional
322 20 dB amplifier installed in its electronics chain in order to compensate for
323 cable losses. As a consequence, this BPM's sensitivity was improved and the
324 impact of the noise and granularity introduced by the digitisers was reduced.

325 Again, these estimates only take into account the noise in the BPMs, but
326 not other effects such as the beam jitter and magnetic fields changes. In
327 fig. 6 we compare the energy readings of BPMs 12 and 24 after the energy
328 calibration. An RMS residual of 4.8 MeV ($1.7 \cdot 10^{-4}$) was found, which is
329 about twice bigger than the noise measurements combined in quadrature.
330 This means that the resolution of the energy measurements of BPMs 12 and
331 24 is, in fact, not limited by the BPM noise alone. Nevertheless, BPMs 12
332 and 24 still allow energy fluctuations to be measured to better than $1.7 \cdot 10^{-4}$,
333 which is well below the expected spectrometer resolution.

334 *3.4. Dipole magnets*

335 An essential prerequisite for the operation of the spectrometer in a Linear
336 Collider is that the beam position downstream of the chicane is not energy
337 dependent, and the upstream beam path is restored downstream. In other
338 words, the chicane has to be symmetric. In a 4-magnet chicane it is also
339 beneficial to match the magnets in each pair producing a parallel translation

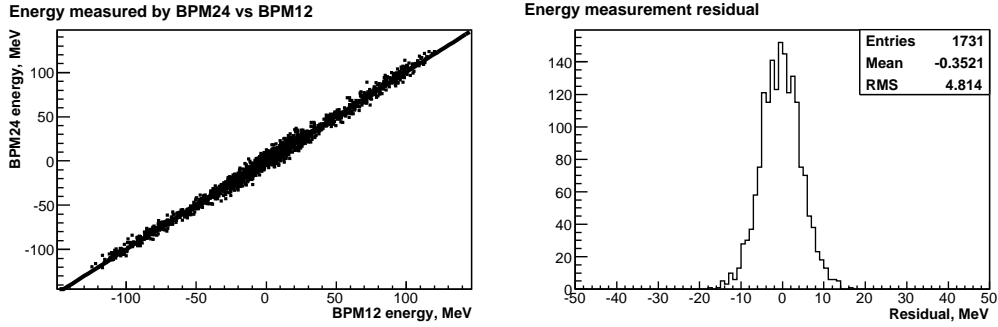


Figure 6: Comparison of BPMs 12 and 24: BPM 24 vs BPM 12 energy measurement (left), residual between BPM 12 and 24 measurements (right).

340 of the beam (a “dogleg”), so that the inclination of the orbit with respect to
 341 the original is kept to a minimum.

342 Magnetic field measurements were performed in March 2007. Some re-
 343 sults are shown in fig. 7. Here, the differences between the measured and
 344 nominal magnetic fields are plotted as a function of the nominal value for
 345 both negative and positive polarities.

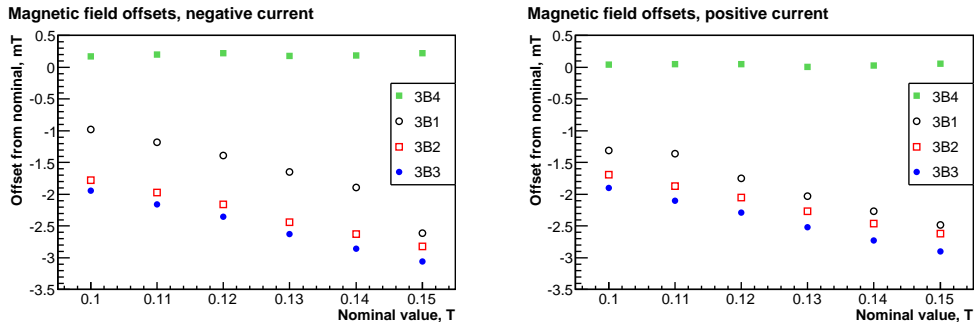


Figure 7: Offsets between the measured and nominal magnetic fields as a function of the nominal value of the four magnets in ESA: Negative current (left); Positive current (right).

346 During these measurements the field of the magnet 3B1 was monitored
 347 with a Hall probe, whereas for the other magnets NMR probes were used. As
 348 can be seen, 3B1, 3B2 and 3B3 follow the same trend, with a difference of
 349 a few tenths of a mT between 3B2 and 3B3, while 3B1 differs by about 1 mT.
 350 Offsets between these magnets can be explained by the individual history and

351 core composition of each (see [6] for details). 3B4 shows a different and much
 352 more consistent behaviour, because only for this magnet a more accurate
 353 relation between the current and the field (as given in [6]) was determined
 354 and used for the field settings. Unfortunately, the analogous measurements
 355 could not be performed for the other magnets due to time constraints.

356 For stability, the magnets were powered by a single supply in ESA, there-
 357 fore, the differences could not be compensated for. As a result, the trajectory
 358 of the beam had a small inclination in the middle of the chicane and was not
 359 fully restored downstream of the chicane, and energy changes were converted
 360 into position variations in BPMs 9, 10 and 11.

361 Using the data from the upstream BPMs the nominal beam position in
 362 the downstream BPMs can be predicted. Considering, for example, BPM 9
 363 measurements after subtraction of the upstream BPMs prediction, we can
 364 recognise the step-like behaviour of the energy during the scan (fig. 8). Note
 365 that, although the net integral field applied to the beam by the chicane is
 366 very small, BPM 9 is still able to resolve the energy changes due to its high
 367 resolution.

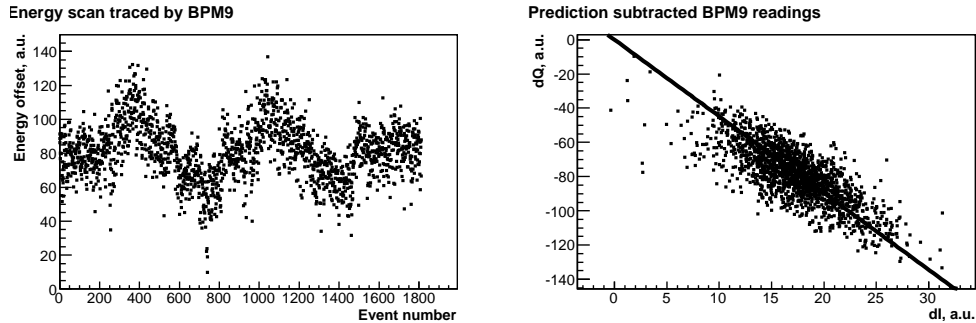


Figure 8: Energy measured by BPM 9 during the scan (left), IQ plot of the measured BPM 9 readings with the predicted readings subtracted (right). The fitted line shows the IQ rotation of the energy measurements.

368 3.5. Energy resolution of the spectrometer

369 The energy measured by the spectrometer can also be predicted by the
 370 energy BPMs 12 and 24. The residual, besides the resolutions of each BPM,
 371 depends on the fluctuations of the magnetic fields, mechanical vibrations, as
 372 well as drifts and other systematic effects and non-linearities.

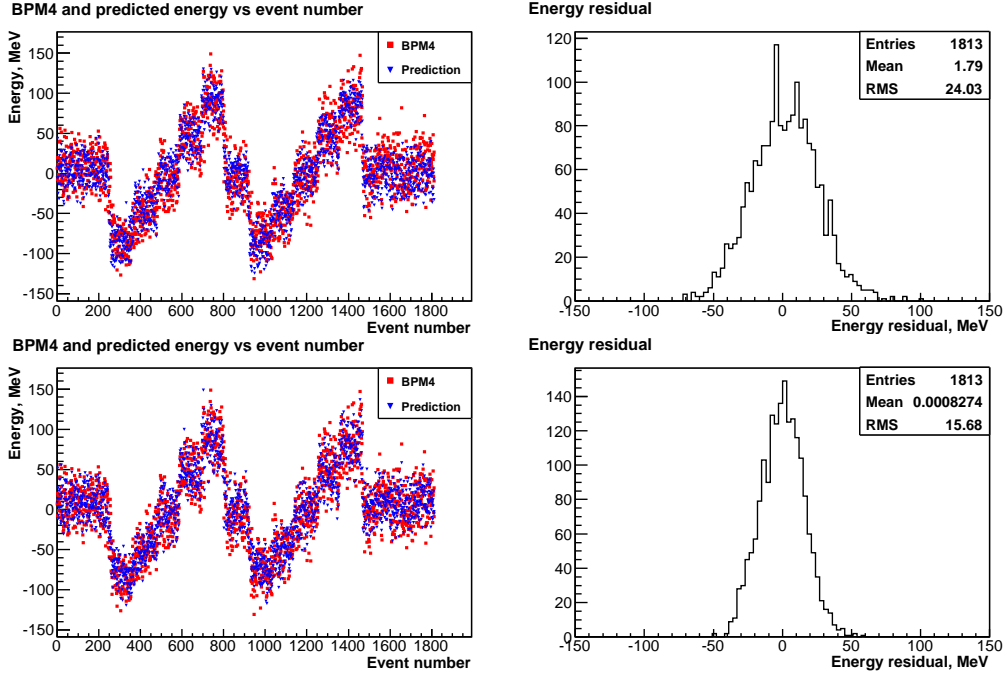


Figure 9: Energy resolution measurement: energy measured by BPM 12 and BPM 4 (top left), residual between BPM 12 and BPM 4 readings (top right), energy measurement predicted by BPMs 12, 24 and additional parameters and BPM 4 reading (bottom left), residual between the prediction and BPM 4 reading (bottom right).

373 We first compare the relative energy measured by BPM 4 with the mea-
 374 surements of BPM 12 (fig. 9, top). This results in a resolution of 24 MeV or
 375 $8.4 \cdot 10^{-4}$. As this is worse than the precision of the orbit reconstruction, we
 376 decided to look for correlations using additional data and applying the SVD
 377 method by starting again from BPM 12 and then adding more data in the
 378 matrix to better reconstruct the spectrometer measurements and understand
 379 the systematics.

380 Each time we added another parameter to the matrix, we re-calculated the
 381 SVD coefficients from the energy scan data and then applied them to the data
 382 from the quiet period. For both data sets we calculated the residual (table 1).
 383 Note that this time when we compare BPM 4 and BPM 12 measurements
 384 the scale is corrected by the SVD for a better match, which results in a lower
 385 residual.

386 Where the residual is improved for both the energy scan and quiet period,

387 we can conclude that the uncertainty associated with the included param-
 388 eter is reduced. We also estimate that uncertainty ($\Delta\sigma/\sigma$) subtracting the
 389 residuals (r) in quadrature and normalising the result by the nominal energy:
 390 $\Delta\sigma/\sigma = \sqrt{(r_{previous}^2 - r_{current}^2)}/E_b$. These estimates are also shown in table 1.

391 The biggest residual reduction is observed when the data from BPMs 9,
 392 10 and 11 are included in the computation. As we know, these BPMs are
 393 sensitive to the energy. In addition, these BPMs outperform the rest of the
 394 BPMs in the beamline by almost an order of magnitude in terms of resolution
 395 [5]. For that reason, even though the net field of the chicane is small, they
 396 form another spectrometer arm with a comparable resolution.

397 Some further improvement is also noted when the bunch charge q , as
 398 measured by one of the reference cavities, is taken into account, even though
 399 all the BPM data were normalised by the charge. This is best explained by
 400 the fact that BPMs 12 and 24, although very sensitive to energy changes, were
 401 not centred in their operating ranges, and were running close to saturation.

402 Ultimately, in order to achieve an energy resolution approaching 10^{-4} ,
 403 one has to monitor the relative motion of the BPMs in the beamline. An
 404 interferometer, once well tuned, seems to be a reliable, fast and precision
 405 tool. Since the mechanical vibrations observed were in the order of a few
 406 hundred nanometres, the Zygo interferometer in our setup only provided a
 407 moderate improvement to the energy measurement.

408 Since our system did not provide bunch-to-bunch magnetic field measure-
 409 ments, only interpolated field data could be used. Inclusion of such data in
 410 the analysis did not provide a consistent improvement, but the data itself
 411 suggests that relatively fast fluctuations of the magnetic field take place.

412 The final result of these investigations is shown in the bottom part of fig. 9.
 413 The resolution was measured to be 15.7 MeV ($5.5 \cdot 10^{-4}$) for an energy scan
 414 and 14.6 MeV ($5.1 \cdot 10^{-4}$) for a quiet period. These numbers are in a good
 415 agreement with the estimate for the precision of the orbit reconstruction of
 416 $5.5 \cdot 10^{-4}$, which means that the weighting of different systematics has been
 417 performed correctly.

418 3.6. *X to Y coupling*

419 Even though the spectrometer chicane operates in the horizontal plane,
 420 the energy scan is also traced in the vertical plane. Firstly, alignment errors
 421 generate a small bend in the vertical direction and, secondly, internal cross-
 422 talk between the x - and y -couplers of the BPMs create a spurious offset in y
 423 due to an offset in x .

Table 1: Energy residuals calculated for BPM 4 including additional parameters. $\Delta\sigma/\sigma$ is the uncertainty calculated as two consequent residuals subtracted in quadrature and normalised by the nominal beam energy.

Data included	Residual, MeV		$\Delta\sigma/\sigma, \times 10^{-4}$	
	energy scan	quiet period	energy scan	quiet period
BPM 12	23.45	21.53	–	–
BPMs 12, 24	23.08	21.64	1.5	0.8 (up)
BPMs 12, 24 and NMR	22.67	22.62	1.5	2.3 (up)
BPMs 12, 24, NMR and fluxgate	22.67	22.62	–	–
BPMs 12, 24, charge (q), NMR and fluxgate	20.52	19.68	3.4	3.9
BPMs 12, 24, 9, 10, 11, q, NMR and fluxgate	15.86	15.26	4.6	4.4
BPMs 12, 24, 9, 10, 11, q, NMR, fluxgate and interferometer	15.68	14.60	0.8	1.6

424 In order to estimate the cross-coupling between the x - and y -coordinates
 425 we again consider the energy scan data, this time to predict the vertical beam
 426 position in BPM 4 using the SVD coefficients obtained from the run with
 427 magnets off. Clearly, as seen in fig. 10 (left), the energy scan is traced in the
 428 measured y -offset. Due to different sensitivities of the x - and y -channels in
 429 BPM 4, we used mover scan data in both directions to get the position scales,
 430 which are used to normalise the raw energy. For that reason the energy is
 431 given in terms of mm in fig. 10. One should, however, keep in mind that
 432 an energy change generates both a different offset and an inclination in the
 433 mid-chicane.

434 The plot on the right-hand side in fig. 10 shows the correlation between
 435 the energy measured in both planes. From the inclination of the line fitting
 436 the data points a rotation of BPM 4 of almost 25° is derived, or an x - y
 437 isolation of about 7.6 dB. Even without tuning, BPMs usually provide an
 438 isolation of 20 dB, which means that the cross-talk can not be explained
 439 solely by the cross-coupling of the signals. At the same time, the rotation is
 440 too large to be caused entirely by the alignment errors. This indicates that
 441 both effects take place. For the future, it is therefore important to minimise
 442 the cross-talk in the BPMs and eliminate fake offsets by careful alignment of
 443 the spectrometer elements.

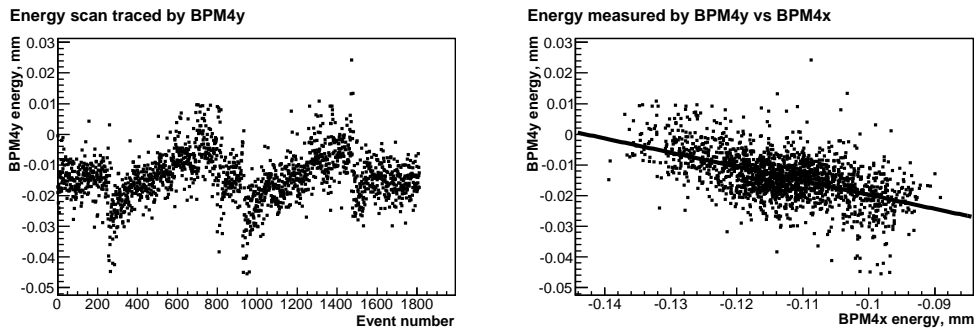


Figure 10: Effect of the chicane on the vertical beam trajectory: energy scan traced by BPM 4 in y (left), energy data measured by BPM 4 in y vs x (right). Position calibration was used to exclude the difference in sensitivities. Hence, the energy is expressed in terms of the offset (mm).

444 4. Suggestions for future experiments

445 Clearly, any improvement of the BPM resolution would have a significant
446 positive impact on both the relative and absolute energy measurement as
447 it reduces the BPM uncertainties contributing to the overall measurement
448 error.

449 Improvement of the internal x - y isolation in the BPMs would also have
450 a positive impact on the energy measurement as the uncertainty introduced
451 by the signal cross-coupled from the orthogonal direction would be smaller.

452 Higher resolution BPMs could also simplify the operation of the spectrom-
453 eter. For a 1 mm dispersion, a resolution of 100 nm would give a 10^{-4} energy
454 uncertainty. Currently, a dynamic range of about 80 dB can be achieved
455 with cavity BPMs, which allows 1 mm offsets to be measured with no need
456 to move the BPMs. Hardware improvements and better algorithms to treat
457 the signals saturating the electronics [14] are expected to expand the dynamic
458 range to 90 and even 100 dB. Additional non-linearities can be calibrated out
459 through a wide range position scan. Hence, systematic effects associated with
460 moving the BPMs to track the beam when the magnets are on can be avoided
461 without compromising the performance.

462 Without the need to move the BPMs when the chicane is in operation,
463 the BPMs are not required to be mounted on precision movers for position
464 calibration purposes, although simpler movers may still be mandatory for
465 calibrating out non-linearities and alignment. A direct calibration of the
466 spectrometer can be performed by changing the phase of the RF in some
467 accelerating modules, as it was done in our ESA experiment. Another way
468 of calibration is to change the magnetic field by a small but known amount
469 and restore the energy scale from the orbit changes.

470 Working with I and Q values of the BPMs directly, we realised that even
471 a 4-magnet chicane does not generate a pure beam offset in the middle of the
472 chicane because of small differences between the magnets. At the required
473 level of precision the inclination still needs to be taken into account. Futher-
474 more, two magnets contribute to the uncertainty of the energy measurement
475 in a 4-magnet chicane.

476 These arguments suggest a revival of the original 3-magnet chicane de-
477 sign as discussed in [4] and shown in fig. 11, where the central magnet, the
478 spectrometer magnet, is instrumented with probes and the other two help
479 to preserve the initial beam trajectory. High-precision BPMs in between the
480 magnets provide information on the bend of the beam, while BPMs upstream

481 of the first magnet predict the default trajectory downstream. In this case,
 482 the spectrometer magnet produces a combination of offset and angle in the
 483 BPMs downstream, but all measured data should still lie on one line in the
 484 IQ space as in our analysis, see section 3.2.

485 Instrumenting the ancillary magnets and extending the interferometer
 486 onto the up- and downstream BPMs would provide redundant energy mea-
 487 surement at a low increment in cost. While the overall resolution is not
 488 expected to become improved as the ancillary magnets operate at half of the
 489 magnetic field of the spectrometer magnet, some systematic effects can be a
 490 priori excluded due to the opposite bend. Also, BPM triplets instead of dou-
 491 blets in between the magnets would also provide redundancy of beam orbit
 492 measurements and improve both the precision and accuracy of the spectrom-
 493 eter.

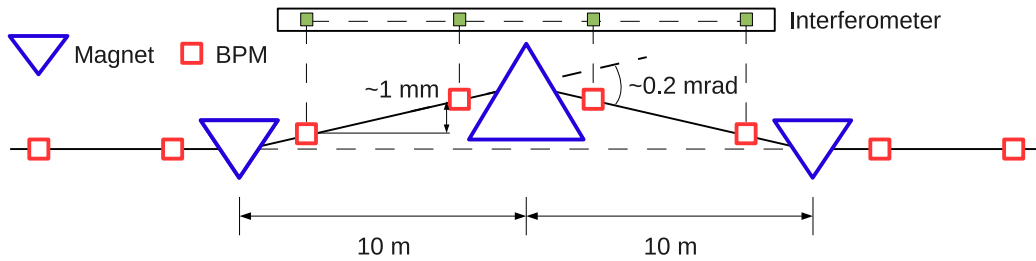


Figure 11: A 3-magnet spectrometer chicane.

494 To predict the default trajectory in a 3-magnet spectrometer, the IQ
 495 space of the BPMs can be scanned by changing the beam deflection of the
 496 ancillary magnets, while the spectrometer magnet is off.

497 A precision interferometer will be required to achieve the 10^{-4} or better
 498 beam energy uncertainty. This becomes critical for a reduced dispersion as
 499 the BPM resolution must be enhanced to 100 nm, since RMS vibrations
 500 measured at ESA were about 300 nm for stationary BPMs and approached
 501 $1 \mu\text{m}$ for BPMs mounted on the movers. The Zygo interferometer fulfils the
 502 requirements of the energy spectrometer, hence the vibrations should not
 503 present a problem in future installations.

504 The resolution of the spectrometer also depends on the availability of
 505 bunch-by-bunch magnetic field measurements. The time resolution of the
 506 NMR probes is in the order of tens of milliseconds, which is sufficient for

507 bunch train averaged measurements in a linear collider, but not for bunch-
508 by-bunch operation. Stabilised low-noise power supplies for the magnets,
509 dedicated readout for each probe (no multiplexing), and combination of NMR
510 and Hall probes will help improve the accuracy of the bunch-by-bunch mea-
511 surements.

512 5. Summary

513 The model-independent analysis of the data obtained with the prototype
514 Linear Collider spectrometer based on a magnetic chicane achieved a single-
515 bunch resolution of $5.5 \cdot 10^{-4}$ using a BPM system with a micrometre level
516 precision of the beam orbit measurements. This value satisfies the require-
517 ments for the Linear Collider in most scenarios, and can be improved. Note,
518 that it should not be mistaken for the absolute accuracy, which requires
519 further studies.

520 An improved BPM resolution is the key factor to enhance the energy
521 resolution. To achieve the 10^{-4} level, stabilisation of the magnetic field in the
522 chicane combined with fast and reliable field measurements and monitoring
523 of the relative BPM motion in the horizontal plane are also mandatory.

524 Novel signal processing and analysis techniques allow the BPM resolution
525 to be pushed to the 100 nm level and below, while enhancing the dynamic
526 range of cavity BPMs beyond the current limit of approximately 80 dB, so
527 that large beam offsets can still be measured. This means that the dispersion
528 in the chicane, and hence the beam emittance degradation caused by the
529 spectrometer, can be significantly reduced. Further improvements of the
530 BPM resolution and their dynamic range would allow operation of the chicane
531 without BPM movers, eliminating associated systematic errors.

532 Working with uncalibrated in-phase and quadrature BPM readings, one
533 does not have to distinguish between the beam angle and offset changes
534 in the middle of a 4-magnet chicane. Both the angle and offset follow the
535 energy changes, and the IQ readings produce a straight line in the IQ plane.
536 However, an energy calibration of the whole system may be required in this
537 case. It is also possible to work with calibrated offsets, providing the chicane
538 magnets are closely matched.

539 For simplicity reasons, a 3-magnet chicane may be a possible configu-
540 ration. In this configuration, the energy calibration of the chicane becomes
541 necessary. Hence, any reference to a well known physics quantity, such as the
542 Z-mass, or a complementary method to measure E_b , is important for both

543 the scale corrections of the relative measurements and establishing the offset
544 for absolute energy measurements.

545 **References**

- 546 [1] J. Brau, (ed.), et al., International Linear Collider reference design
547 report, Volume 2: Physics at the ILC, ILC Global Design Effort and
548 World Wide Study, ILC-REPORT-2007-001 (2007).
- 549 [2] J. Brau, (ed.), et al., International Linear Collider reference design
550 report, Volume 3: Accelerator, ILC Global Design Effort and World
551 Wide Study, ILC-REPORT-2007-001 (2007).
- 552 [3] R. Assmann, et al., Calibration of centre-of-mass energies at LEP2 for
553 a precise measurement of the W boson mass, *Eur. Phys. J. C*39 (2005)
554 253–292.
- 555 [4] V. N. Duginov, et al., The beam energy spectrometer at the Interna-
556 tional Linear Collider, DESY LC Note, LC-DET-2004-031 (2004).
- 557 [5] M. Slater, et al., Cavity BPM system tests for the ILC energy spec-
558 trometer, *Nucl. Instrum. Meth. A*592 (2008) 201–217.
- 559 [6] M. Viti, Precise and fast beam energy measurement at the International
560 Linear Collider, Ph.D. thesis, Humboldt-Universitaet zu Berlin, DESY-
561 THESIS-2010-007, 2010.
- 562 [7] M. Hildreth, et al., Linear Collider – BPM-based energy spectrometer,
563 SLAC ESA Test Beam Proposals (2004, 2006).
- 564 [8] F. C. Demerest, High-resolution, high-speed, low data age uncertainty
565 heterodyne displacement measuring interferometer electronics, *Meas.*
566 *Sci. Technol.* 9 (1998) 1024–1030.
- 567 [9] H. J. Schreiber, et al., Magnetic measurements and simulations of a
568 4-magnet dipole chicane for the International Linear Collider, Particle
569 Accelerator Conference (PAC07), Albuquerque, NM, USA (2007).
- 570 [10] S. Kostromin, M. Viti, Magnetic measurements for magnets 10D37,
571 ILC-SLACESA Note, TN-2008-1 (2008).

- 572 [11] N. R. B., et al., The Stanford Two-Mile Accelerator, Benjamin, New
573 York, 1968.
- 574 [12] A. Lyapin, et al., A Prototype S-Band Cavity BPM System for the ILC
575 Energy Spectrometer, EUROTeV Report, 2008-072 (2008).
- 576 [13] W. H. Press, et al., Numerical Recipes in C, Cambridge University
577 Press, 1992.
- 578 [14] S. Boogert, et al., Cavity beam position monitor system for ATF2,
579 International Particle Accelerator Conference (IPAC 10), Kyoto, Japan
580 (2010).